Resilience of MSE Walls with Marginal Backfill under a Changing Climate: Quantitative Assessment for Extreme Precipitation Events

Farshid Vahedifard, M.ASCE[1]; Faraz S. Tehrani[2]; Vahid Galavi[3]; Elisa Ragno[4]; and Amir AghaKouchak, M.ASCE[5]

Abstract: Climate change is expected to alter statistics of extreme events in the future. Adapting geotechnical infrastructure to a changing climate necessitates quantitative assessment of the potential climate change impacts on the performance of infrastructure. This study numerically investigates the hydromechanical response of a mechanically stabilized earth (MSE) wall constructed with marginal backfill to extreme rainfall events under a changing climate. The need for investigating the effects of extreme precipitation on marginal backfill is more pronounced because larger matric suction can be developed in such backfills. To address this need, this paper compares the performance of an MSE wall using two sets of rainfall intensity-duration-frequency (IDF) curves, denoted as *baseline* and *projected*, for the Seattle area. The baseline IDF curves are provided by the National Oceanic and Atmospheric Administration (NOAA) and currently used for design purposes, and the projected IDF curves are obtained using 20 climate model simulations of the future. The results show that use of the baseline IDFs can lead to underestimation of the wall deformation and loads carried by reinforcements. The results highlight the importance of site-specific assessments to quantify the potential impacts of climate change on the performance of current and future MSE walls. Such consideration gains even more importance considering the increasing interest in using marginal backfills in earth retaining structures due to economic and environmental considerations. **DOI: 10.1061/(ASCE)GT.1943-5606.0001743.**

Author keywords: Climate change; Soil stabilization; Geosynthetics; Marginal backfill; Unsaturated soils; Suction; Extreme precipitations; Numerical modeling; Nonstationary extreme value analysis (NEVA).

Introduction

Recent evidence suggests future changes in frequency and/or severity of climatic extreme events caused or intensified by anthropogenic climate change (e.g., USGCRP 2009; EEA 2012; IPCC 2012; NOAA 2013; NRC 2013). Increasing trends have been reported for average surface temperature, intensity of extreme precipitation events, sea levels, and storm severity in the United States and in other parts of the world (Karl et al. 2009; IPCC 2012; Kunkel et al. 2013; Hao et al. 2013). Even concurrent and compounding extreme events have increased substantially in recent decades (Hao et al. 2013; Mazdiyasni and AghaKouchak 2015; Wahl et al. 2015). These climate trends unfavorably influence existing natural and artificial geotechnical structures by exposing them to drying, soil desiccation, shrinkage, fluctuation in the groundwater table, significant erosion, and highly dynamic pore pressure changes (e.g., CACC 2015; Vardon 2015; Vahedifard et al. 2015a, 2016d; Robinson and Vahedifard 2016; Robinson et al. 2017). The imposed impacts can threaten the integrity of geotechnical structures and lead to various modes of failure such as uplift, subsidence, piping, internal erosion, and slope instability (e.g., NRC 2008; Crozier 2010; Taylor et al. 2013; Vardon 2015).

Among recent climate trends, increased intensity of extreme precipitation is recognized as one of the major causes of several catastrophic failures in natural and engineered earth structures, leading to casualties and major economic losses in some cases (e.g., NRC 2008; Crozier 2010; Coe and Godt 2012; Yoo 2013). The U.S. Global Change Research Program reported that the amount of precipitation falling in the heaviest 1% of rain events has increased by approximately 20% in the U.S. during the past 50 years (Karl and Knight 1998; Groisman et al. 2005; USGCRP 2009). Table 1 shows the increase in amounts of very heavy precipitation which were reported in different regions of the U.S. from 1958 to 2007 (USGCRP 2009).

Although several large-scale studies have been conducted to evaluate various aspects and implications of climate change, there is a clear gap in the knowledge in terms of quantitative and structural-scale assessment of the performance of geotechnical infrastructure under observed and projected climate trends. This assessment requires quantifying the impact of climate change on the two factors governing the response of geotechnical infrastructure to climate extremes: supplies (e.g., shear strength and compressibility of soil) and demands (e.g., loads imposed on the structure due to climate extremes). Such quantitative studies can help to properly evaluate the failure risk and resilience of current earth structures and to safely design future earth structures for a changing climate. For this purpose, the geotechnical engineering community needs to

[1]Assistant Professor, Dept. of Civil and Environmental Engineering, Mississippi State Univ., Mississippi State, MS 39762 (corresponding author). E-mail: farshid@cee.msstate.edu

[2]Researcher and Consultant, Dept. of Geoengineering, Deltares, 2629 HV, Delft, Netherlands. E-mail: faraz.tehrani@deltares.nl

[3]Researcher and Consultant, Dept. of Geoengineering, Deltares, 2629 HV, Delft, Netherlands. E-mail: vahid.galavi@deltares.nl

[4]Ph.D. Student, Dept. of Civil and Environmental Engineering, Univ. of California, Irvine, CA 92697. E-mail: ragnoe@uci.edu

[5]Associate Professor, Dept. of Civil and Environmental Engineering, Univ. of California, Irvine, CA 92697. E-mail: amir.a@uci.edu

Note. This manuscript was submitted on May 2, 2016; approved on March 6, 2017; published online on June 1, 2017. Discussion period open until November 1, 2017; separate discussions must be submitted for individual papers. This paper is part of the ***Journal of Geotechnical and Geoenvironmental Engineering***, © ASCE, ISSN 1090-0241.

Table 1. Increases in Amounts of Very Heavy Precipitation from 1958 to 2007 in the United States (Data from USGCRP 2009)

Region	Percent change
Northeast	67
Midwest	31
Southeast	20
Great plains	15
Northwest	16
Southwest	9
Hawaii	12
Alaska	23

closely collaborate with other related disciplines, including climate change scientists, to specifically address the following questions (e.g., CACC 2015; Vahedifard et al. 2016d): (1) How does climate change and variability affect recurrence intervals of climatic extremes? (2) How does soil behavior vary under thermohydromechanical processes imposed by changes in extremes? and (3) How do climate extremes affect the short-term and long-term behavior of geotechnical structures?

This study investigates the impact of increased rain intensity from changing climate on the performance of mechanically stabilized earth (MSE) walls built with marginal backfill. Mechanically stabilized earth walls have become an integrated component of several critical infrastructures such as bridges, roads, and railroads. This study quantitatively compares the hydromechanical response of MSE walls with marginal backfill for historical (hereafter denoted as *baseline*) and future (hereafter denoted as *projected*) precipitation. The latter is the outcome of global climate model simulations based on prescribed future greenhouse gas emission scenarios. Rainfall intensities for the baseline and projected scenarios are then used in a series of fully coupled stress-unsaturated flow finite element (FE) simulations, and the differences in terms of the wall deformation and reinforcement loads are compared.

MSE Walls and Extreme Precipitation

Severe rainfall events result in substantial and unprecedented changes in the degree of saturation within the unsaturated backfill of MSE walls, which can lead to failure of these structures (Yoo and Jung 2006; Kim and Borden 2013; Koerner and Koerner 2013; Valentine 2013; Yoo 2013; McKelvey et al. 2015). Recent surveys (Koerner and Koerner 2013; Valentine 2013) show that more than 60% of failures and poor performance of MSE walls are caused by internal or external water. Drainage systems for MSE walls are designed based on the expected rainfall intensity with a certain return period. The frequency of an extreme event with a certain return period is typically based on fitting a distribution function to historical data assuming time-invariant parameters, also known as the stationary assumption (Cheng et al. 2014; Katz 2010). The so-called stationary assumption for frequency analysis ignores potential changes in rainfall intensity over time due to climate change and variability. If the rainfall intensity increases over time, the drainage system may not function as intended, thus potentially increasing the degree of saturation of the backfill.

Although some of the reported water-induced failures in MSE walls have been due to poor drainage and the subsequent saturation of the backfill, many failures were reported in unsaturated MSE walls under varying moisture content conditions (Koerner and Koerner 2013; Valentine 2013). It is well known that changes in pore water pressure and matric suction have a very important effect on the stability of soil masses, including reinforced and nonreinforced soil structures. In MSE walls, drainage systems and, in some cases, waterproofing membranes are included in order to reduce the pore water pressure in the soil. Excessive pore water pressure developed in the backfill due to unprecedented rainfall events and/or lack of proper drainage capacity can threaten the integrity of a MSE wall. In conventional design, the matric suction is regarded as a redundancy factor and therefore it is usually ignored. As demonstrated through numerical simulations and field experiments of reinforced soil walls and slopes, matric suction, which contributes to the soil's shear strength, can significantly increase the soil-reinforcement interface strength and can reduce the load mobilized in the reinforcement (e.g., Iyro and Rowe 2005; Riccio et al. 2014; Thuo et al. 2015; Vahedifard et al. 2016c). However, increases in degree of saturation and the associated loss of suction during extreme rain events will lead to abrupt increases in active earth pressures, which significantly increase the reinforcement load in marginal backfills (Yoo and Jung 2006; Vahedifard et al. 2014, 2015b, 2016c). The corresponding decrease in effective stress will also lead to a decrease in the pullout resistance (e.g., Hatami and Esmaili 2015). It may also lead to an increased creep as the retained load reaches closer to the ultimate pullout resistance. Such changes, if not properly accounted for, may threaten the integrity of MSE walls and can lead to catastrophic failures.

Incidence of several precipitation-induced failures in MSE walls (e.g., Yoo and Jung 2006; Kim and Borden 2013; Koerner and Koerner 2013; Valentine 2013; Yoo 2013; McKelvey et al. 2015) highlights a crucial need for consideration of increased rain intensity due to climate change in analysis of existing MSE walls as well as in design of future MSE walls. This need is more pronounced for MSE walls with a marginal backfill (i.e., backfill with high fines content). In design guidelines such as FHWA (2009) used by the public sector, the allowable fines content (i.e., passing sieve #200) for MSE walls is limited to 15%. The allowable fines content is higher for walls which are designed and built in the private sector. For example, the National Concrete Masonry Association (NCMA 2010) allows up to 35% fines content; this limit can be as high as 50% if a geotechnical engineer is involved in the design. Recently there has been an increasing interest in the use of marginal backfills from local materials, which contain higher fines content, because of their environmental and economic advantages (e.g., Yoo and Jung 2006; Miyata and Bathurst 2007; Marr and Stulgis 2012; Kim and Borden 2013; Portelinha et al. 2013; Esmaili et al. 2014; Thuo et al. 2015). The presence of higher fines content can significantly decrease the permeability and can also lead to development of considerably large matric suction in marginal backfills.

Historical and Future Precipitation Intensity-Duration-Frequency Curves

Design of geotechnical infrastructure relies on observed historical extremes such as rainfall and flood records. In most parts of the world, infrastructure (e.g., dams, MSE walls, drainage systems, and levees) design is based on intensity-duration-frequency (IDF) curves (e.g., Sugahara et al. 2009; Madsen et al. 2009; Simonovic and Peck 2009). For different combinations of rainfall duration (e.g., 1-day and 2-day) and intensity, IDF curves provide return-period information (i.e., how often on average different combinations of duration-intensity are expected to occur). The current methods solely rely on historical information, assuming a stationary climate, meaning statistics of extreme rainfall events are not expected to change significantly over time. Intensity-duration-frequency curves are typically derived by fitting a representative distribution function, such as the generalized extreme value

(GEV) distribution, to annual rainfall maximums for different durations (e.g., 1-h, 1-day, 2-day).

In the commonly used stationary assumption, the parameters of the fitted distribution are assumed to be constant over time (Jacob 2013). However, ground-based observations in the U.S. (Table 1) and many other regions across the world indicate increases in extreme rainfall events (Karl et al. 2009; Hao et al. 2013; Groisman et al. 2005, 2012; Kunkel et al. 2013; DeGaetano 2009; Cheng et al. 2014). Furthermore, model simulations indicate plausible changes in future extreme events (IPCC 2012), due to anthropogenic emissions and the corresponding expected warming (Trenberth 2011). In a warmer climate, the atmospheric water holding capacity will increase, leading to more water vapor in the atmosphere (Min et al. 2011; IPCC 2013). More water vapor in the atmosphere could increase the likelihood of extreme rainfall events (Kunkel et al. 2013; Emori and Brown 2005), and consequently lead to higher flood risk (Das et al. 2011; Jongman et al. 2014). This indicates that the statistics of rainfall extremes may change over time, a concept termed nonstationarity (Jacob 2013; Cheng et al. 2014; Cooley 2013).

The authors argue that because of the observed and expected increases in extreme events in a warming climate, infrastructure design concepts should be re-evaluated (Cheng and AghaKouchak 2014; Vahedifard et al. 2016a, d). This paper uses projected IDF curves to assess the response of MSE walls in a changing climate and compares the results with those obtained using the baseline IDF curves based on the stationary assumption.

Theory of Unsaturated Seepage-Stress Coupling

This paper performs a fully coupled fluid flow-deformation analysis using the commercial FE code *PLAXIS* to simultaneously analyze deformations and pore pressures of the modeled MSE wall under steady and transient unsaturated flow conditions. The coupled formulation is based on Biot's theory (Biot 1941) which includes the equilibrium equation and the continuity equation of the soil-water mixture. The Mohr–Coulomb failure criterion and the van Genuchten–Mualem model (van Genuchten 1980; Mualem 1976) are employed as mechanical and hydraulic models, respectively.

The van Genuchten–Mualem model is defined as

$$S = S_{\text{res}} + (S_{\text{sat}} - S_{\text{res}})\left[1 + \left(g_a\left|\frac{p_w}{\gamma_w}\right|\right)^{g_n}\right]^{(1-g_n)/g_n} \tag{1}$$

where S = degree of saturation at a given pore water pressure p_w; S_{res} = residual saturation; S_{sat} = water saturation at saturated conditions; g_a and g_n = soil water characteristic curve (SWCC) fitting parameters; and γ_w = unit weight of water. As defined, g_a is related to the air entry value and g_n is a function of the rate of water extraction from the soil once the air entry value has been exceeded.

Bishop's effective stress (Bishop and Blight 1963), defined by the following relationship, is used in the coupled analysis to determine the shear strength of unsaturated soils:

$$\underline{\sigma} = \underline{\sigma}' + \underline{m}[\chi p_w + (1-\chi)p_a] \tag{2}$$

where $\underline{\sigma}$ = total stress vector (Voigt notation); $\underline{\sigma}'$ = effective stress vector; p_a = pore air pressure; $\underline{m}$ = vector containing components that are equal to 1 for the normal stresses and 0 for the shear stresses; and χ = effective stress parameter called matric suction coefficient which varies between 0 and 1 to cover a range from dry to fully saturated soils. The matric suction coefficient χ is generally determined experimentally and it depends on the degree of saturation, porosity, and matric suction $(p_a - p_w)$ of the soil sample (e.g., Bolzon et al. 1996; Bishop and Blight 1963). Experimental evidence on the matric suction coefficient χ is quite scarce. The effective stress parameter χ is set to the effective degree of saturation, S_e, to properly account for the variation of effective stress due to a change in saturation. The effective degree of saturation is defined as

$$S_e = \frac{S - S_{\text{res}}}{S_{\text{sat}} - S_{\text{res}}} \tag{3}$$

The matric suction can be simplified for practical application assuming that the pore air pressure is constant and is small enough to be neglected (i.e., $p_a \approx 0$). Therefore the matric suction is equal to the pore water pressure with an opposite sign. The effective suction is defined as

$$\psi_{\text{eff}} = -S_e(p_a - p_w) \tag{4}$$

which is the contribution of the matric suction in the effective stress, i.e.

$$\underline{\sigma} = \underline{\sigma}' + \underline{m}(p_a + \psi_{\text{eff}}) \tag{5}$$

The Richards equation (Richards 1931) can be used to describe unsaturated flow in a porous medium as

$$\underline{q} = \frac{k_{\text{rel}}}{\rho_w g}\underline{\underline{k}}_{\text{sat}}(\nabla p_w + \rho_w \underline{g}) \tag{6}$$

where $\underline{q}$ = vector of specific discharge; $\underline{\underline{k}}_{\text{sat}}$ = permeability matrix in the saturated state; ρ_w = water density; ∇p_w = gradient of the pore water pressure that causes the water to flow; $\underline{g}$ = vector of gravitational acceleration; and k_{rel} = relative permeability, defined as the ratio of the permeability at a given saturation to $\underline{\underline{k}}_{\text{sat}}$. The van Genuchten hydraulic model defines k_{rel} as

$$k_{\text{rel}} = S_s^{g_l}\left[1 - (1 - S_e^{g_n/(g_n-1)})^{(g_n-1)/g_n}\right]^2 \tag{7}$$

where g_l = fitting parameter.

Using a form of the Richards equation (Galavi et al. 2009) and by neglecting the compressibility of solid particles, the continuity equation for transient flow conditions can be written as

$$-n\left(\frac{S}{K_w} - \frac{\partial S}{\partial p_w}\right)\frac{\partial p_w}{\partial t} + \nabla^T \underline{q} = 0 \tag{8}$$

where n = porosity of the soil; S = degree of saturation; K_w = bulk modulus of water; and $\nabla^T \underline{q}$ = divergence of the specific discharge.

Numerical Modeling

Geometry of Model

This study numerically simulates a geosynthetic reinforced wall of height $H = 5.4$ m using the commercial FE code *PLAXIS*. Fig. 1 shows a schematic of the MSE wall considered in this study. The soil model is discretized with 15-noded plane-strain triangular elements. The wall is reinforced with 4.75-m structural geogrids, which are installed at variable vertical spacings (Fig. 1) starting from $z = 20.2$ m (the toe of the wall is at elevation $z_{\text{toe}} = 20$ m). The wall facing with 8° batter angle is assumed to be constructed with segmental concrete blocks with 0.2 m height and 0.3 m depth. The concrete block has a unit weight of

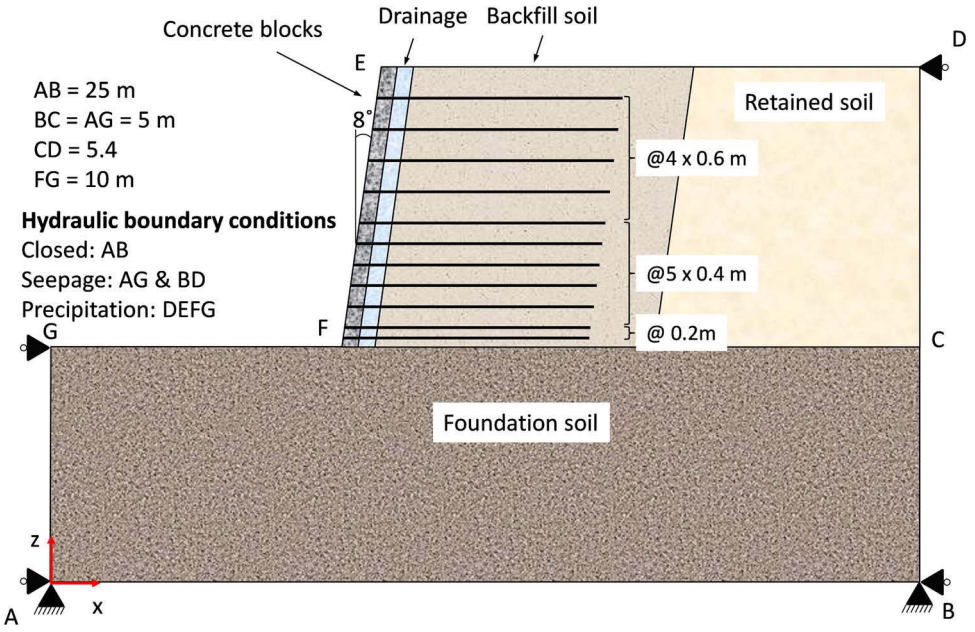

Fig. 1. Geometry of the model MSE wall used in this study

24 kN/m^3, Young's modulus of 30 GPa, and Poisson's ratio of 0.3. The wall is constructed on a competent foundation soil. The water table is assumed to be very deep.

Soil and Reinforcement Parameters

Soil Properties

A backfill soil with high fines content (over 30% of fines passing a number 200 sieve) is considered in the numerical model. The suction magnitude is directly related to fines content. Soil was modeled using the Mohr-Coulomb (MC) constitutive model. The strength and flow parameters of the backfill soil were deduced from Yoo and Jung (2006). Table 2 lists the properties of the soil used in the verification analysis.

The SWCC and the hydraulic conductivity function (HCF) for the backfill used in the analysis are shown in Fig. 2. The SWCC and HCF used in the current study were reported by Yoo and Jung (2006) for a similar marginal backfill. It was assumed that the retained soil shared the same hydraulic parameters with the backfill material. For the foundation soil, $g_n = 3$ and $g_a = 3$ m^{-1} were used in the analyses, whereas for the drainage soil, $g_n = 2.68$ and $g_a = 14.5$ m^{-1} were used in the analyses. For all soils, it was assumed that $S_{sat} = 1.0$. For all soils, $g_l = 0.5$ was used.

Reinforcements

Geogrid elements in *PLAXIS* were used to model layers of the structural geogrids with the tensile modulus of 250 kN/m; minimum rib thickness of 0.76 mm, which was taken as the thickness of the geogrid; and tensile strengths of 4.1 and 8.5 kN/m for axial strains of 2 and 5%, respectively. A rigid interface was considered between the geogrids and the backfill soil. To ensure zero axial load at the end point of reinforcements, the interface element between the soil and the reinforcement was slightly (5 mm) extended into the soil.

Interface Elements

The interfaces of soil and structural elements were defined using the MC model. Two types of interfaces were defined in the numerical model to properly accommodate the interaction of soil and structural elements, namely the facing plates and geogrids. The following equation defines the interface strength properties between soil and structural elements:

$$\Lambda_{\text{interface}} = R_{\text{interface}}\Lambda_{\text{soil}} \tag{9}$$

where Λ = corresponding strength parameter (e.g., friction); and $R_{\text{interface}}$ = reduction factor. For soil-facing interfaces, the reduction factor was set to 0.7, whereas for soil-geogrid interfaces no reduction was set (i.e., $R_{\text{interface}} = 1.0$). It is noted that because the shear

Table 2. Soil Properties Used in the FE Analyses

Model parameter	Backfill soil	Drainage	Retained soil	Foundation soil
Dry unit weight, γ_d (kN/m^3)	15.71	19.00	15.71	18.85
Saturated unit weight, γ_{sat} (kN/m^3)	19.64	20.00	19.64	22.80
Void ratio, e	0.667	0.55	0.667	0.5
Elastic modulus, E (MN/m^2)	15	30	10	110
Poisson's ratio, ν	0.3	0.3	0.3	0.3
Friction angle, φ' (degrees)	22	45	22	45
Dilatancy angle, ψ (degrees)	0	15	0	15
Cohesion, c' (kPa)	13	1	5	15
Saturated hydraulic conductivity, $\underline{\underline{k}}_{sat}(i,i)$ (m/day)[a]	0.0432	20	0.0432	2.0

[a]The saturated hydraulic conductivity is assumed identical in both x and z directions.

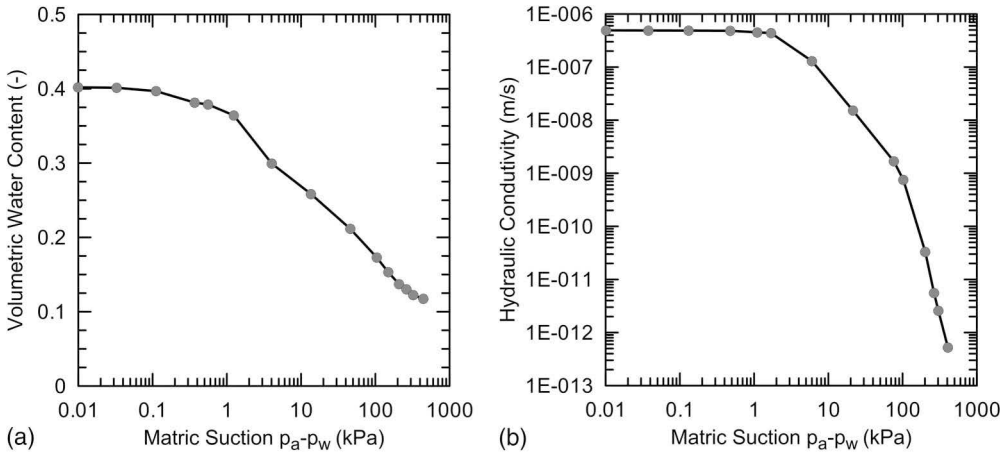

Fig. 2. SWCC and HCF of the backfill used in the numerical analyses: (a) SWCC; (b) HCF (modified from Yoo and Jung 2006, © ASCE)

strength of the soil will change by any changes in matric suction, the soil-geogrid interface strength will also vary by changes in matric suction. For the block-block interface, an interface angle of friction of 35° was used.

Past and Future Extreme Precipitation Events

Seattle was selected as the study area to investigate the impact of future extreme precipitation on geotechnical infrastructures design. Historical (1950–1999) and future (2050–2099) daily precipitation available from Climate Model Intercomparison Project Phase 5 (CMIP5; Taylor et al. 2013) were employed as input for deriving IDF curves to assess the response of MSE walls in a changing climate. The future precipitation time series were obtained from 20 climatic models formed by the Representative Concentration Pathways 8.5 (Taylor et al. 2013) emission scenario, which is also known as the high emission future scenario.

Following the National Oceanic and Atmospheric Administration (NOAA) Atlas 14 (Bonnin et al. 2006) guidelines, annual maximums for different durations were extracted from historical and future precipitation simulations and the GEV distribution was used for frequency analysis. The GEV cumulative distribution function can be expressed as (Coles et al. 2001)

$$\Psi(x) = \exp\left\{-\left[1+\xi\left(\frac{x-\mu}{\sigma}\right)\right]^{-1/\xi}\right\} \tag{10}$$

where $\Psi(x)$ is defined for $1+\xi[(x-\mu)/\sigma] > 0$; elsewhere, $\Psi(x)$ is either 0 or 1 (Coles et al. 2001). The distribution is defined by the location parameter (μ) that represents the center of the distribution, the scale parameter (σ) that represents the deviation around μ, and the shape parameter (ξ) that describes the behavior of the distribution's tail. Extreme value analysis and parameter estimation were performed using the *Nonstationary Extreme Value Analysis* (NEVA; Cheng et al. 2014) software which allows for both stationary and nonstationary extreme value assessment. Current IDF curves, provided by NOAA and used for practical applications, were obtained under the stationary assumption. To be consistent with the current IDF curves procedure, the same methodology was applied to derive the baseline IDF curves, meaning that the distribution parameters μ, σ, and ξ were assumed to be time invariant (i.e., stationary). Typically, climate model simulations are bias adjusted based on observations. The IDF curves from historical simulations were bias corrected based on the current NOAA IDF curves such that the baseline IDF curves were identical to what is currently used in practical applications.

To derive IDF curves from future precipitation, when there was a trend in the data a nonstationary approach was used for frequency analysis. Following Cheng et al. (2014), upon detection of a statistical significant trend (Mann–Kendall trend test at a 95% confidence level) in the time series of annual precipitation extremes, the GEV parameters were estimated using a time-dependent location parameter [e.g., $\mu(t)=\mu_1 t+\mu_0$, where t is the time in years, and μ_0 and μ_1 are regression parameters] and constant σ and ξ parameters. In the NEVA framework, a Bayesian approach is implemented to estimate the model parameters along with their uncertainty bounds. For more information about IDF curve analysis under stationary and nonstationary assumptions, refer to Cheng and AghaKouchak (2014). The same bias correction ratio applied to the baseline simulations is also applied to future IDF curves assuming climate model biases are similar in the future (i.e., a common approach is used in bias correction of climate models). This study used Seattle's historical and future precipitation simulations to obtain the baseline and projected IDF curves as explained previously.

When IDF curves were retrieved under the nonstationary assumption, the time-variant parameter $\tilde{\mu}$ was derived as the temporal median of $\mu(t)$. Consequently, the precipitation intensities (q_p) were derived as follows:

$$q_p = \left[\left(-\frac{1}{\ln p}\right)^{\xi} - 1\right] \times \frac{\sigma}{\xi} + \tilde{\mu}, \qquad (\xi \neq 0) \tag{11}$$

Fig. 3(a) displays the baseline IDF curves provided by NOAA. Historical and future precipitations from 20 separate CMIP5 climate model simulations were used to project current IDFs into the future (projected IDFs), where each single point represents an ensemble mean for a given duration and return period. In addition to the median, for each duration and return period, the 5th percentile (lower bound) and 95th percentile (upper bound) of the 20 climate models were obtained. Figs. 3(b–d) depict lower bound, median, and upper bound of the projected IDF curves, respectively. As shown, for different durations, the projected IDF curves were higher than their corresponding baseline curves, meaning that the baseline IDF curves underestimate the expected extremes. For example, the median and upper bound projected 1-day rainfall intensities for the 50-year recurrence interval were approximately 26 and 65%, respectively, greater than the baseline intensities. On the other

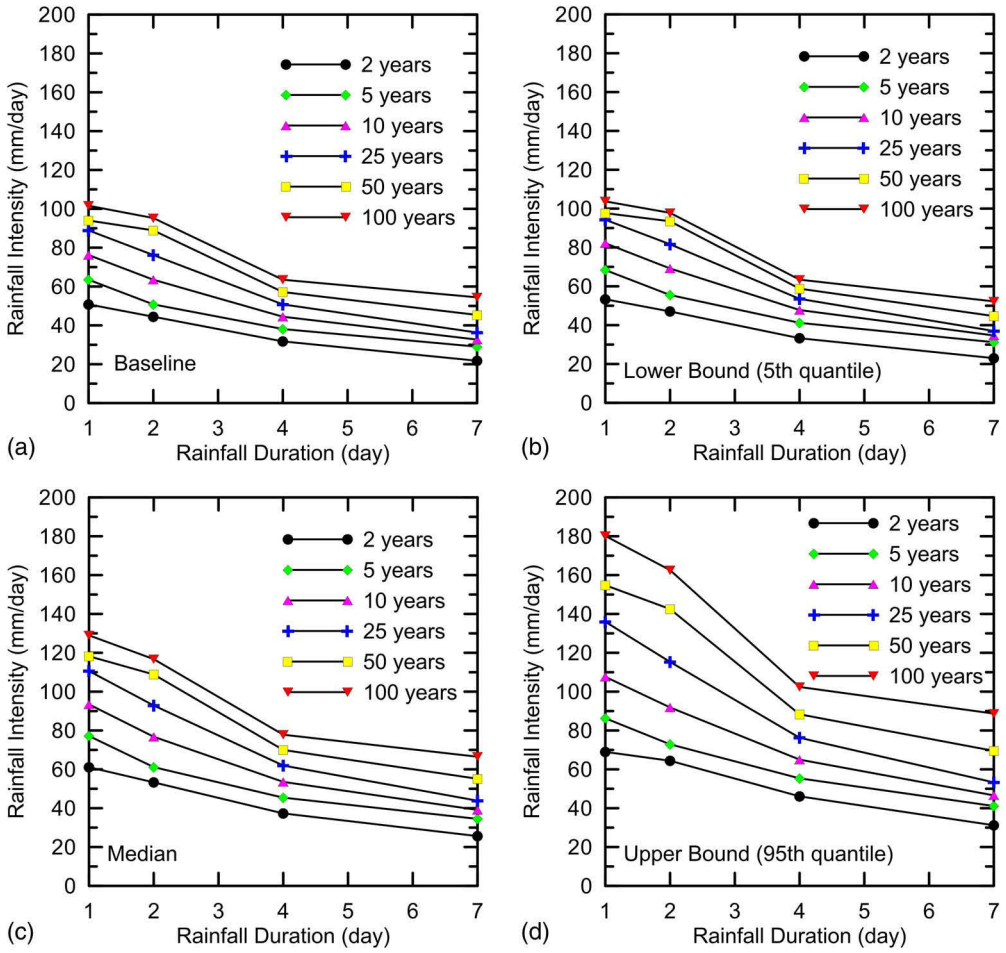

Fig. 3. Precipitation IDF curves for the Seattle area: (a) baseline; (b) lower bound projected; (c) median projected; (d) upper bound projected

hand, compared with the baseline data, the 7-day rainfall intensities were approximately 22 and 53% higher in the median and upper bound projected IDF curves. It should be noted that climate model simulations are subject to biases and uncertainties (Liu et al. 2014). For this reason, climate change assessment is typically based on relative change (here, precipitation extremes) in the projection and baseline periods (i.e., the difference between projection and baseline periods).

Initial Mechanical and Flow Conditions

Referring to Fig. 1, the boundary AB is fixed in both x and z directions, whereas the boundaries AG and BD are fixed only in the x direction. To specify the flow boundary conditions, the boundary AB is set as a closed boundary against flow, whereas the boundaries AG and BD are taken as seepage boundaries. The infiltration was simulated by assigning the precipitation boundary condition to the boundaries GF, FE, and ED. The precipitation boundary condition is a mixed boundary condition in which water inflow with a known quantity (i.e., rainfall intensity) under certain conditions is allowed.

To simulate the drainage behind the wall, a gravel strip of width 30 cm and length equal to the height of the wall was chosen behind the segmental blocks. It should be noted that the segmental blocks and the associated interfaces were impermeable, and therefore acted as closed boundaries, whereas the geogrids and their interfaces were permeable.

Modeling Stages

The simulation for the baseline and projected models consisted of three phases:

- Phase 1: construction of the wall, performed in 27 stages such that at every stage 0.2 m of the wall was constructed;
- Phase 2: generation of a uniform suction throughout the soil domain that was used as the initial hydraulic condition ($t = 0$) for the subsequent transient seepage analysis; and
- Phase 3: transient seepage using the corresponding 1-day and 7-day precipitation extremes with return period of 50 years ($t = 1$ day to $t = 7$ days).

To examine the effects of initial suction, two sets of analyses were performed: one set with initial suction of 60 kPa, which was reported by Yoo and Jung (2006) for a similar marginal backfill, and a second set with initial suction of 240 kPa. It is noted that much larger suctions can possibly be developed in marginal fills under certain circumstances (e.g., prolonged droughts). A heavy rain after or in the middle of a prolonged drought has been reported in several cases and can impose a more critical scenario to earthen structures including MSE walls (e.g., Vahedifard et al. 2015a, 2016d; Robinson and Vahedifard 2016). Such a case involves a multihazard analysis including consecutive extreme events (i.e., drought followed by a heavy rain). Although it is an interesting case which warrants further investigation, it is beyond the scope of the current study which aims to investigate the performance of MSE walls only under extreme precipitation.

Once the initial hydraulic condition was achieved, a transient seepage analysis (Phase 3) was conducted by imposing the baseline and projected rainfall intensities. In order to investigate the effect of rain duration on the performance of the wall, 1-day and 7-day rains with 50-year return period were considered in the analyses. Therefore the following analyses were carried out after Phase 2:

1. 1-day baseline heavy rainfall with 93.98 mm/day intensity;
2. 1-day projected heavy rainfall with 154.79 mm/day intensity;

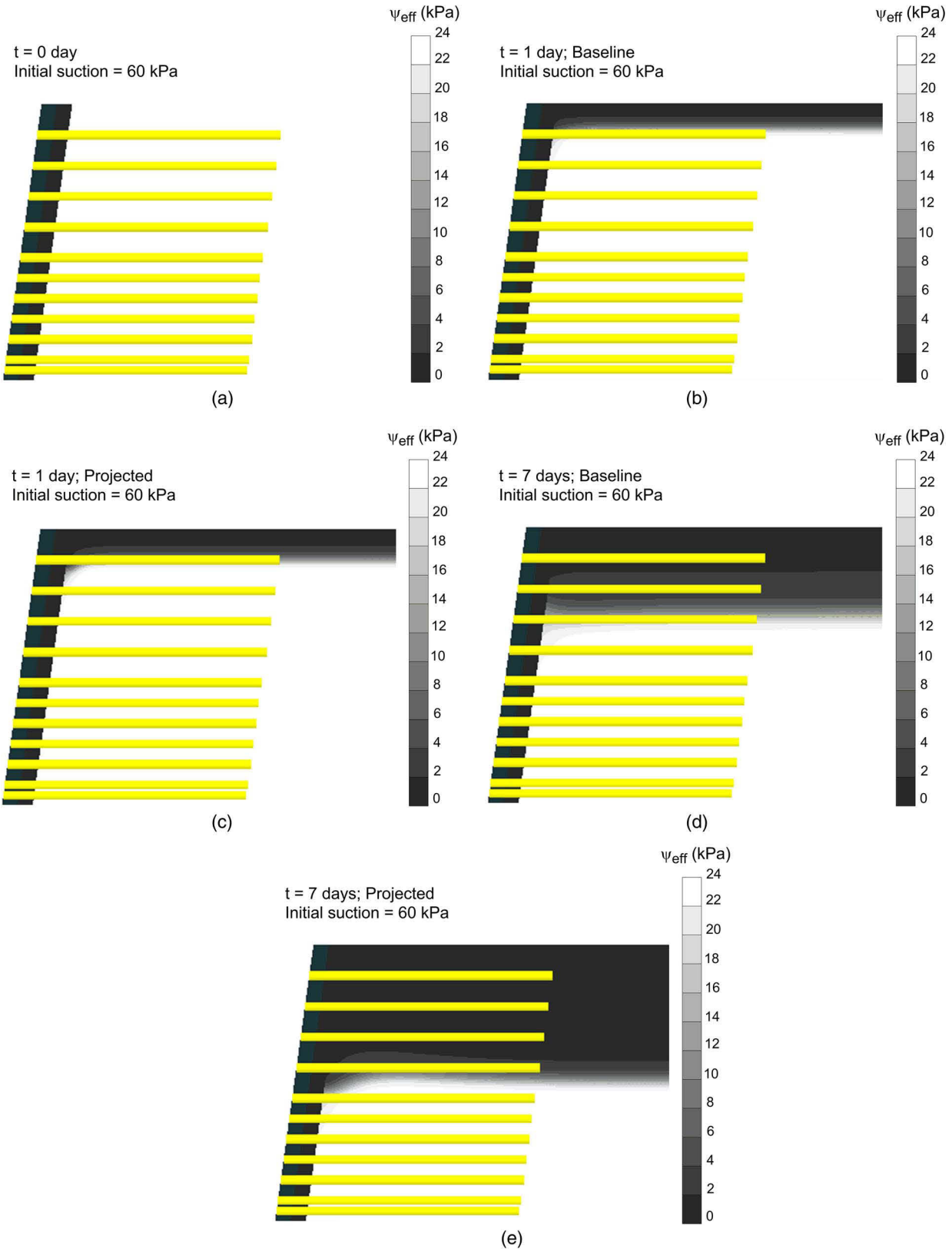

Fig. 4. Contours of effective suction for initial suction of 60 kPa: (a) initial condition; (b) 1-day baseline rain; (c) 1-day projected rain; (d) 7-day baseline rain; (e) 7-day projected rain

3. 7-day baseline heavy rainfall with 45.36 mm/day intensity; and
4. 7-day projected heavy rainfall with 69.49 mm/day intensity.

The projected IDF curves considered in the analyses were associated with the upper bound (95th percentile) from all IDF curves derived based on 20 climate model simulations as a measure of the most extreme conditions in the future [Fig. 3(d)]. Because the change in the median of the projected rainfall relative to the historical simulations did not show considerable effects on the performance of the MSE wall, this paper focuses only on the upper bound of the projected rainfalls relative to the baseline [Fig. 3(a)].

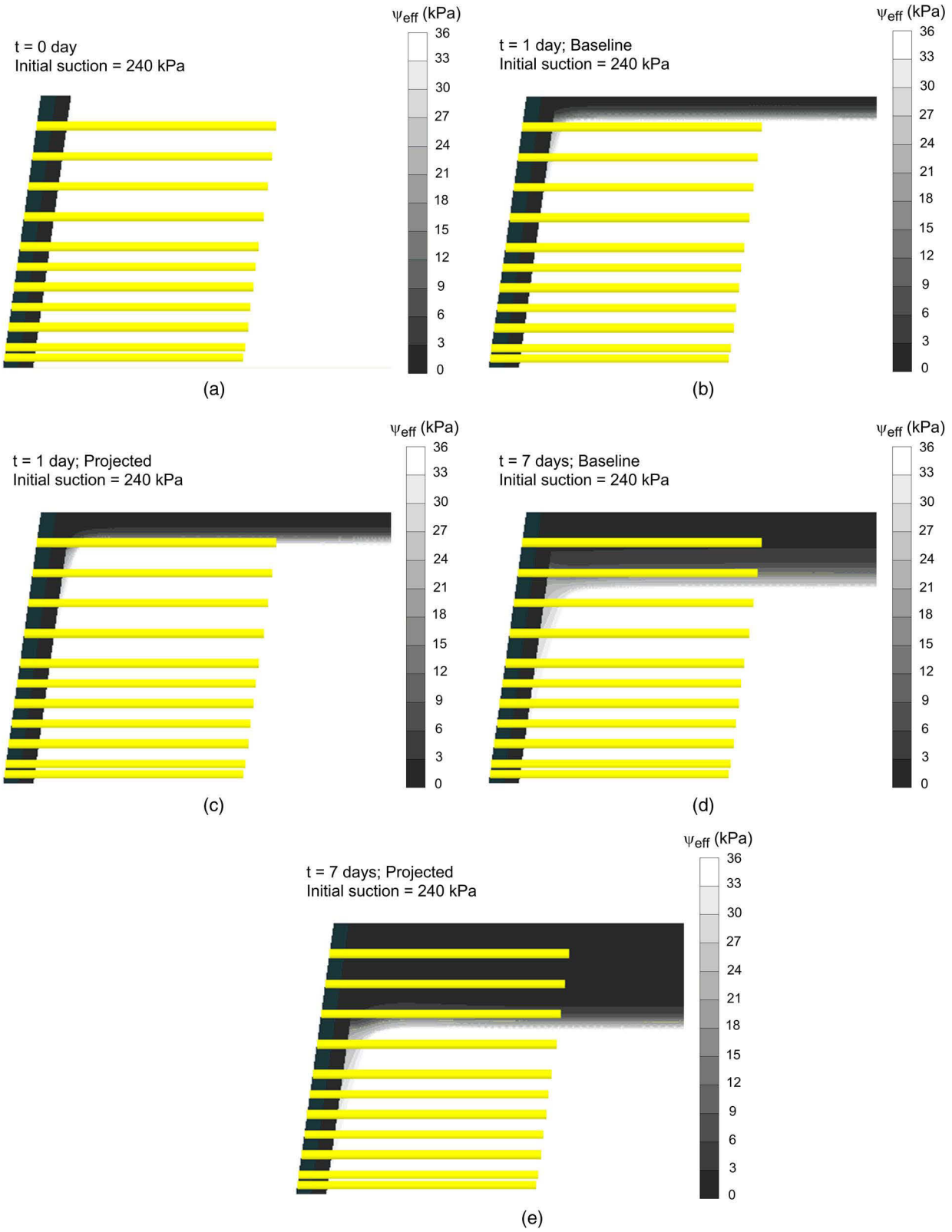

Fig. 5. Contours of effective suction for initial suction of 240 kPa: (a) initial condition; (b) 1-day baseline rain; (c) 1-day projected rain; (d) 7-day baseline rain; (e) 7-day projected rain

Results and Discussions

This section explains and discusses the results of the numerical analyses of the effect of baseline and projected heavy rainfalls on the performance of the wall. The impacts of the two types of precipitation extremes are compared in terms of the effective suction generated across the soil domain, effective saturation, mean effective stress, wall displacement, and reinforcement loads.

Figs. 4 and 5 illustrate the influence of the simulated baseline and projected rainfalls on the soil effective suction under transient unsaturated flow conditions for initial suctions of 60 kPa and 240 kPa, respectively. To further examine the change in the effective suction behind the wall, a cross section of the backfill soil located 2 m behind the wall ($x - x_{toe} = 2$ m) is selected. The effective suction profile and the relative change in effective suction due to climatic changes for 1-day and 7-day rains are depicted in Fig. 6. It is clear from Figs. 4–6 that the effect of baseline rainfalls (after 1 day and 7 days) on the effective suction across the soil domain was less than that of the projected rainfalls. Among all rainfalls, the 7-day projected rainfall had the maximum effect on the change in the effective suction.

Fig. 7 shows the effect of simulated rainfalls on the soil effective saturation behind the wall ($x - x_{toe} = 2$ m). Similar to what was seen for the effective suction, the degree of saturation was also significantly affected by the change in the model rainfalls as well as initial suction. This effect was more notable for 7-day rainfalls, in which up to 157% change in effective degree of saturation was reached behind the wall when the initial suction is 60 kPa. Such an increase is even greater for the case with initial suction of 240 kPa, where up to 667% change in effective degree of saturation was reached behind the wall. Figs. 7 and 6 along with Figs. 3(a and d) show that a 53% increase in 7-day rainfall with a 50-year return period resulted in the maximum of 157% (for 60 kPa initial suction) and 667% (for 240 kPa initial suction) increases in the soil effective saturation behind the wall, which yielded up to 100% decreases in the effective suction for soil not very close to the wall crest. For the 1-day rainfall, the increase of the rainfall intensity by as much as 65% resulted in the maximum of 80% (for 60 kPa initial suction) and 165% (for 240 kPa initial suction) increases in soil effective saturation, which in turn yielded up to 100% decrease in the effective suction for both initial suction values (the few centimeters below the wall crest which is under the effect of water ponding

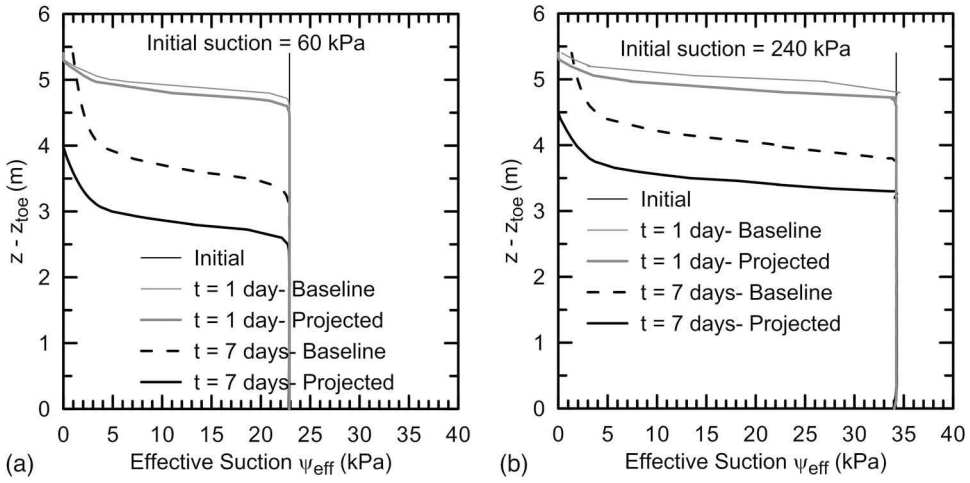

Fig. 6. Effect of change in intensity and duration of rain behind the wall ($x - x_{toe} = 2$ m) on effective suction with initial suction of (a) 60 kPa; (b) 240 kPa

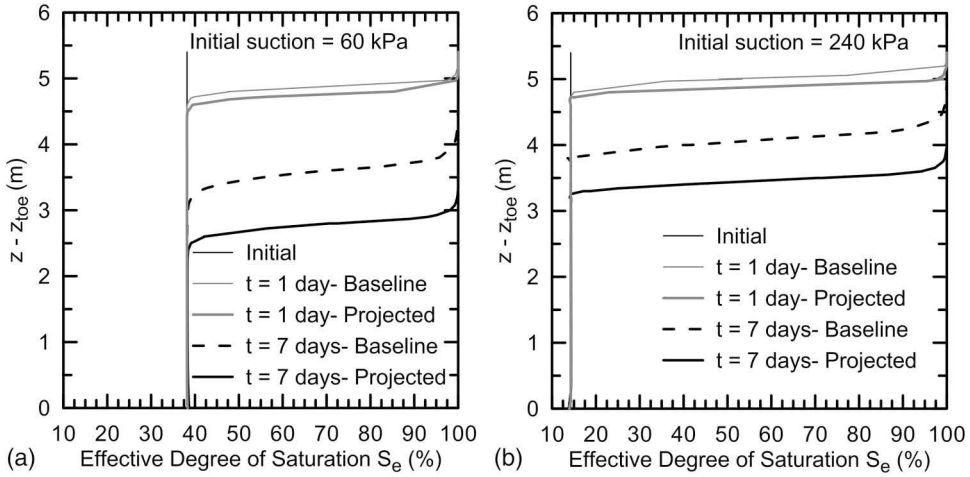

Fig. 7. Effect of rainfall intensity and duration behind the wall ($x - x_{toe} = 2$ m) on effective degree of saturation with initial suction of (a) 60 kPa; (b) 240 kPa

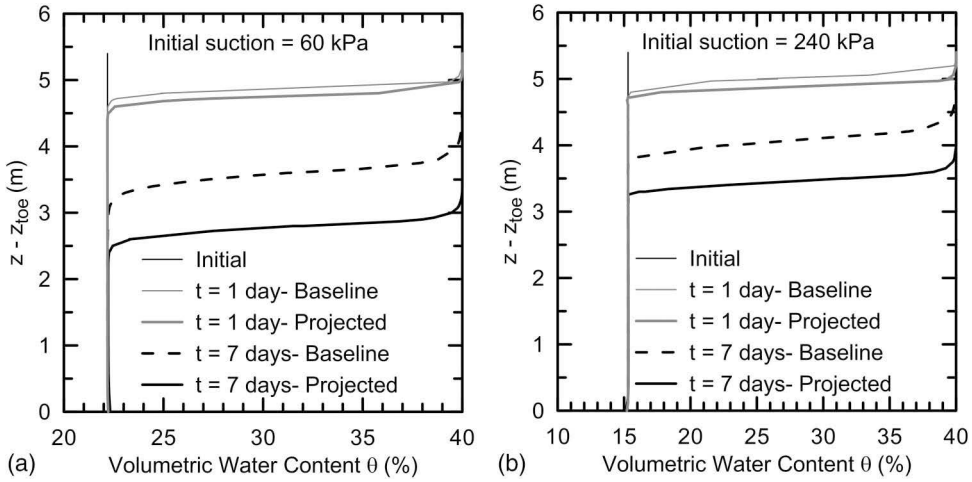

Fig. 8. Effect of rain on change in the volumetric water content for initial suction of (a) 60 kPa; (b) 240 kPa

is neglected in this comparison). This decrease in the effective suction implies reduction in the shear strength of the backfill soil, which can affect the mechanical performance of the wall. The shear strength of unsaturated soils is primarily controlled by the effective stress.

Once the effective stress is determined, one can calculate the corresponding shear strength of unsaturated soil (e.g., Lu and Likos 2006; Vahedifard and Robinson 2016; Vahedifard et al. 2016b). Figs. 8 and 9 depict the effect of rainfall intensities and initial suction on the volumetric water content and mean effective stress behind the wall ($x - x_{toe} = 2$ m), respectively. As shown in Fig. 9, the mean effective stress significantly decreased behind the wall when the soil was subjected to precipitation. The change in the mean effective stress became more pronounced as the rainfall intensity and duration (notable for 7-day rainfalls) increases. Such a decrease in the mean effective stress is an indication of higher loss of shear strength behind the wall when the rain intensity and duration increase. It is worth mentioning that for both initial suctions of 60 and 240 kPa, significant ponding took place on the wall crest for the 7-day projected rainfall. The effect of this ponding (additional weight of water) is clearly reflected in the increase in the mean effective stress of the soil at the bottom of the wall.

The effect of simulated baseline and projected precipitation extremes on the mechanical performance of the wall is illustrated in Figs. 10 and 11 which depict the wall horizontal displacement (u_x) and maximum reinforcement loads T_{max}, respectively. Fig. 10 shows that the wall horizontal displacement corresponding to the projected rainfalls was significantly greater than that corresponding to baseline rainfalls. The difference between the two at the top of the wall with initial suction of 60 kPa reached 232 and 89% for 1-day and 7-day precipitations, respectively. The difference at the top of the wall with initial suction of 240 kPa reached 44 and 63% for 1-day and 7-day precipitations, respectively.

The difference in the performance of the wall was also observed in the maximum loads T_{max} mobilized in the geogrid reinforcements as shown in Fig. 11. The shear strength of the soil due to matric suctions was significantly reduced upon suction attenuation. The reduction in matric suction due to higher rainfall intensity showed its effect in the maximum reinforcement loads which, for the wall with 60 kPa initial suction, increased up to 6 and 60% after 1- and 7-day heavy precipitations, respectively. This increase for the wall with 240 kPa initial suction was up to 35 and 51% after 1-day and 7-day heavy precipitations, respectively.

This study was intended to quantify the impact of climate change on extreme precipitation, and subsequently on the

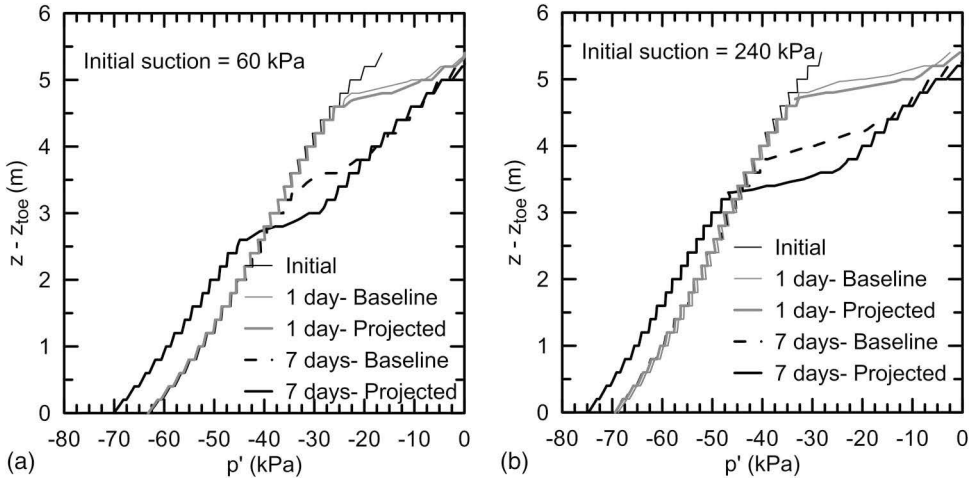

Fig. 9. Effect of rain on change in the mean effective stress for initial suction of (a) 60 kPa; (b) 240 kPa

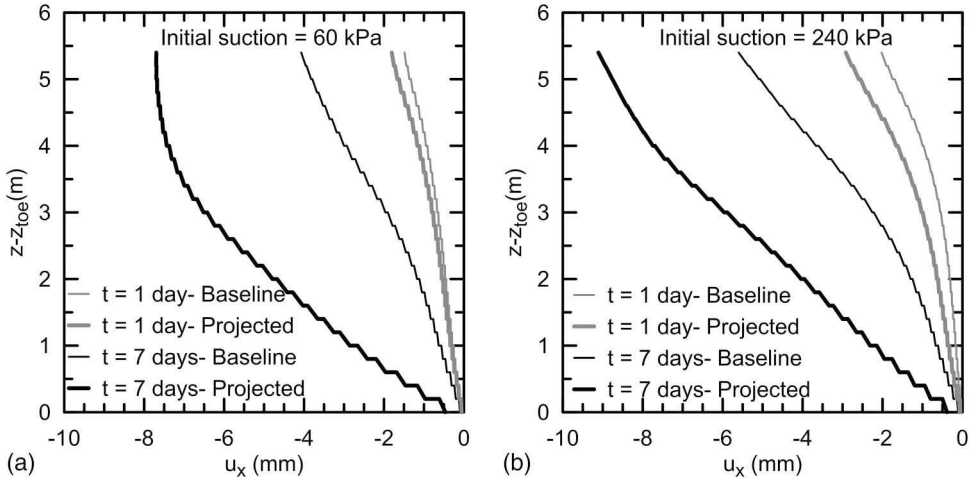

Fig. 10. Effect of rainfall intensity, duration and initial suction on the displacement of the wall: (a) displaced wall with initial suction of 60 kPa; (b) displaced wall with initial suction of 240 kPa

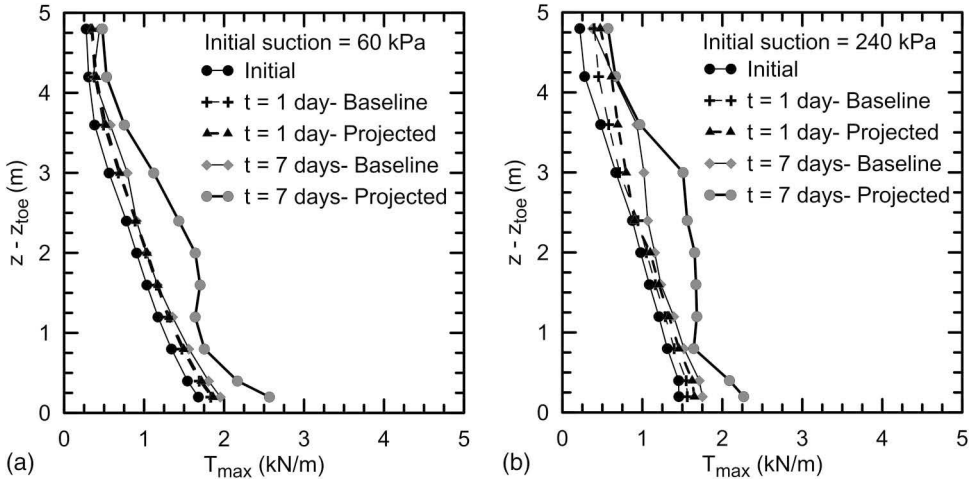

Fig. 11. Effect of change in intensity and duration of rain on the maximum reinforcement loads T_{max}: (a) maximum reinforcement load for initial suction of 60 kPa; (b) maximum reinforcement load for initial suction of 240 kPa

hydromechanical response of an MSE wall in terms of deformation, reinforcement loads, and so on. The authors do not suggest whether or not this impact is significant, but rather propose employing similar site-specific analyses based on the study area, earthen structure, and climatic extreme of interest. Although this paper used a specific region (Seattle), the proposed methodology can be used for other regions and earthen structures. Although the impact can be insignificant in one region/earthen structure, it might be significant in another area/earthen structure. For example, as shown in Table 1, the amount of very heavy precipitation in the southwestern United States increased only 9% from 1958 to 2007, but in the same period the increase was as much as 67% in the northeastern United States. For MSE walls, the adverse impacts of increased rain due to climate change can be safely handled with well-designed and properly constructed internal/external drainage systems and waterproofing membranes. However, for other critical earthen structures, such as levees, reducing adverse effects can be more challenging and warrants further investigation. This paper integrated geotechnical engineering with hydrology and climate science to quantify how climate change–induced changes in extreme precipitations may affect the coupled performance of a critical geotechnical structure (i.e., MSE walls). The modeling approach introduced in this paper can be applied to other natural or engineered earthen structures (e.g., levees), regions, and climate extremes to address the direct impacts of climate change on geotechnical infrastructure. Following such an approach can potentially provide an opportunity for the broader geotechnical engineering community to investigate whether climate change matters to geotechnical engineering and to what degree.

Conclusions

Mechanically stabilized earth walls have become a major part of critical infrastructure in different sectors. Evidence of increased rain intensity due to climate change as well as occurrence of several precipitation-induced failures in MSE walls emphasize the need to assess the resilience of MSE walls in a changing climate. Increased rain intensity increases the degree of saturation of unsaturated backfill, leading to a reduction in soil suction and soil strength and an increase in earth pressures behind the wall and reinforcement loads.

This study quantitatively compared the performance of an MSE wall built with marginal backfill in Seattle area based on (1) historical (baseline) rainfall extremes and (2) future (projected) extreme rainfall considering a warming climate. The baseline and projected IDF curves were used in a series of fully coupled stress-unsaturated flow FE simulations of an MSE wall and the differences were compared.

The behavior of the modeled MSE wall was monitored at the end of construction under two initial uniform suctions followed by a transient infiltration under expected extreme rainfall events in a changing climate. The analyses were performed on a wall constructed with marginal backfill (with high fines content) due to rapidly increasing interest in using marginal backfills in construction of MSE walls to reduce construction costs. The behavior of the modeled wall at 1-day and 7-day rainfall durations obtained for a 50-year recurrence interval were compared in terms of effective suction and effective degree of saturation of the backfill soil and wall displacement and maximum reinforcement loads.

For the study area selected for this study, the analyses did not show substantial impacts on the performance of the modeled MSE wall when considering the median of the future precipitation extremes relative to the historical baseline rainfall. The presented model did, however, indicate that the impact can be significant when considering the 95th percentile of the projected precipitation extremes from climate models. It is imperative to consider the aforementioned precipitation extremes to ensure that geotechnical structures are safe and competent. The results showed that the upper part of the wall was highly influenced by both baseline and projected extremes, whereas the lower part of the wall did not show any notable and yet meaningful response to change in the rain intensity. The greater influence of the rain on the upper part of the wall was attributed to the hydraulic properties of the marginal backfill used in the FE analyses. It was also observed that the duration of rain also could be a determining factor in the performance of MSE walls. Furthermore, it was shown that the wall with higher initial suction was influenced more by the extreme rainfalls than was the wall with lower initial suction.

The results highlight the importance of assessing potential impacts of climate change and variability on the performance of MSE walls. Such consideration gains even more importance considering the fact that marginal backfills are becoming an attractive choice for geotechnical and structural engineers in design and construction of MSE walls. Although this paper studied a specific region (Seattle), the proposed methodology can be adopted for other regions as well as other natural and engineered earthen structures.

Acknowledgments

This material is based upon work supported in part by the National Science Foundation under Grants Nos. CMMI-1634748 and CMMI-1635797. Any opinions, findings, and conclusions or recommendations expressed in this material are those of the authors and do not necessarily reflect the views of the National Science Foundation. We acknowledge the World Climate Research Programme's Working Group on Coupled Modelling, which is responsible for CMIP, and we thank the climate modeling groups for producing and making available their model output. For CMIP the U.S. Department of Energy's Program for Climate Model Diagnosis and Intercomparison provides coordinating support and led development of software infrastructure in partnership with the Global Organization for Earth System Science Portals.

References

Biot, M. A. (1941). "General theory of three-dimensional consolidation." *J. Appl. Phys.*, 12(2), 155–164.

Bishop, A. W., and Blight, A. K. G. (1963). "Some aspects of effective stress in saturated and partially saturated soils." *Géotechnique*, 13(3), 177–197.

Bolzon, G., Schrefler, B. A., and Zienkiewicz, O. C. (1996). "Elastoplastic soil constitutive laws generalised to partially saturated states." *Géotechnique*, 46(2), 279–289.

Bonnin, G. M., Martin, D., Lin, B., Parzybok, T., Yekta, M., and Riley, D. (2006). "Precipitation-frequency atlas of the United States." *NOAA Atlas 14*, U.S. Dept. of Commerce, National Oceanic and Atmospheric Administration, National Weather Service, Silver Spring, MD, 1–65.

CACC (Committee on Adaptation to a Changing Climate). (2015). *Adapting infrastructure and civil engineering practice to a changing climate*, J. R. Olsen, ed., ASCE, Reston, VA.

Cheng, L., and AghaKouchak, A. (2014). "Nonstationary precipitation intensity-duration-frequency curves for infrastructure design in a changing climate." *Sci. Rep.*, 4, 7093.

Cheng, L., AghaKouchak, A., Gilleland, E., and Katz, R. W. (2014). "Non-stationary extreme value analysis in a changing climate." *Clim. Change*, 127(2), 353–369.

Coe, J. A., and Godt, J. W. (2012). "Review of approaches for assessing the impact of climate change on landslide hazards." *Proc., 11th Int. and 2nd North American Symp. on Landslides and Engineered Slopes*, Banff, Canada, E. Eberhardt, C. Froese, A. K. Turner, and S. Leroueil, eds., Vol. 1, Taylor & Francis Group, London, 371–377.

Coles, S., Bawa, J., Trenner, L., and Dorazio, P. (2001). *An introduction to statistical modeling of extreme values*, Springer, London.

Cooley, D. (2013). "Return periods and return levels under climate change." *Extremes in a changing climate*, Springer, Dordrecht, Netherlands, 97–114.

Crozier, M. J. (2010). "Deciphering the effect of climate change on landslide activity: A review." *Geomorphology*, 124(3–4), 260–267.

Das, T., Dettinger, M. D., Cayan, D. R., and Hidalgo, H. G. (2011). "Potential increase in floods in California's Sierra Nevada under future climate projections." *Clim. Change*, 109(S1), 71–94.

DeGaetano, A. T. (2009). "Time-dependent changes in extreme-precipitation return-period amounts in the continental United States." *J. Appl. Meteorol.*, 48(10), 2086–2099.

EEA (European Environment Agency). (2012). "Climate change, impacts and vulnerability in Europe 2012: An indicator-based report." Copenhagen, Denmark.

Emori, S., and Brown, S. J. (2005). "Dynamic and thermodynamic changes in mean and extreme precipitation under changed climate." *Geophys. Res. Lett.*, 32(17), L17706.

Esmaili, D., Hatami, K., and Miller, G. A. (2014). "Influence of matric suction on geotextile reinforcement marginal soil interface strength." *Geotext. Geomembr.*, 42(2), 139–153.

Federal Highway Administration (FHWA). (2009). "Mechanically stabilized earth walls and reinforced soil slopes design and construction guidelines—Vol II." *Technical Rep. FHWA-NHI-10-025*, Washington, DC.

Galavi, V., Brinkgreve, R. B. J., Bonnier, P. G., and Gonzalez, N. A. (2009). "Fully coupled hydro-mechanical analysis of unsaturated soils." *Proc., 1st Int. Symp. on Computational Geomechanics (ComGeo I)*, International Center of Computational Engineering (IC2E), Rhodes, Greece, 486–495.

Groisman, P. Y., Knight, R. W., Easterling, D. R., Karl, T. R., Hegerl, G. C., and Razuvaev, V. N. (2005). "Trends in intense precipitation in the climate record." *J. Clim.*, 18(9), 1326–1350.

Groisman, P. Y., Knight, R. W., and Karl, T. R. (2012). "Changes in intense precipitation over the central United States." *J. Hydrometeorol.*, 13(1), 47–66.

Hao, Z., AghaKouchak, A., and Phillips, T. J. (2013). "Changes in concurrent monthly precipitation and temperature extremes." *Environ. Res. Lett.*, 8(3), 034014.

Hatami, K., and Esmaili, K. (2015). "Unsaturated soil-woven geotextile interface strength properties from small-scale pullout and interface tests." *Geosynthetics Int.*, 22(2), 161–172.

IPCC (Intergovernmental Panel on Climate Change). (2012). "Managing the risks of extreme events and disasters to advance climate change adaptation." *A Special Rep. of Working Groups I and II of the Intergovernmental Panel on Climate Change*, C. B. Field, et al., eds., Cambridge University Press, Cambridge, U.K., 582.

IPCC (Intergovernmental Panel on Climate Change). (2013). "Climate change 2013. The physical science basis." *Working Group I Contribution to the Fifth Assessment Rep. of the Intergovernmental Panel on Climate Change—Abstract for decision-makers*, World Meteorological Organization, Geneva.

Iryo, T., and Rowe, R. K. (2005). "Infiltration into an embankment reinforced by nonwoven geotextiles." *Can. Geotech. J.*, 42(4), 1145–1159.

Jacob, D. (2013). "Nonstationarity in extremes and engineering design." *Extremes Changing Clim.*, Springer, Dordrecht, Netherland, 363–417.

Jongman, B., et al. (2014). "Increasing stress on disaster risk finance due to large floods." *Nat. Clim. Change*, 4(4), 264–268.

Karl, T. R., and Knight, R. W. (1998). "Secular trends of precipitation amount, frequency, and intensity in the United States." *Bull. Am. Meteorol. Soc.*, 79(2), 231–241.

Karl, T. R., Melillo, J. M., and Peterson, T. C. (2009). *Global climate change impacts in the United States*, Cambridge University Press, New York.

Katz, R. (2010). "Statistics of extremes in climate change." *Clim. Change*, 100(1), 71–76.

Kim, S. K., and Borden, R. H. (2013). "Numerical simulation of MSE wall behavior induced by surface-water infiltration." *J. Geotech. Geoenviron. Eng.*, 10.1061/(ASCE)GT.1943-5606.0000927, 2110–2124.

Koerner, R. M., and Koerner, G. R. (2013). "A data base, statistics and recommendations regarding 171 failed geosynthetic reinforced mechanically stabilized earth (MSE) walls." *Geotext. Geomemb.*, 40, 20–27.

Kunkel, K. E., et al. (2013). "Monitoring and understanding trends in extreme storms: State of knowledge." *Bull. Am. Meteorol. Soc.*, 94(4), 499–514.

Liu, Z., Mehran, A., Phillips, T. J., and AghaKouchak, A. (2014). "Seasonal and regional biases in CMIP5 precipitation simulations." *Climate Research*, 60(1), 35–50.

Lu, N., and Likos, W. J. (2006). "Suction stress characteristic curve for unsaturated soil." *J. Geotech. Geoenviron. Eng.*, 10.1061/(ASCE)1090-0241(2006)132:2(131), 131–142.

Madsen, H., Arnbjerg-Nielsen, K., and Mikkelsen, P. S. (2009). "Update of regional intensity-duration–frequency curves in Denmark: Tendency towards increased storm intensities." *Atmos. Res.*, 92(3), 343–349.

Marr, A., and Stulgis, R. P. (2012). "Selecting backfill materials for MSE retaining walls." *Draft Final Rep. NCHRP 24-22*, Geotesting Express, Inc., Acton, MA.

Mazdiyasni, O., and AghaKouchak, A. (2015). "Substantial increase in concurrent droughts and heatwaves in the United States." *Proc. Nat. Acad. Sci.*, 112(37), 11484–11489.

McKelvey, J. A., Khabbazian, M., and Van Keuren, D. J. (2015). "Hydraulic performance of mechanically stabilized earth structures." *Proc. Geosynthetics 2015*, Portland, Oregon, Industrial Fabrics Association International, Roseville, MN.

Min, S. K., Zhang, X., Zwiers, F. W., and Hegerl, G. C. (2011). "Human contribution to more-intense precipitation extremes." *Nature*, 470(7334), 378–381.

Miyata, Y., and Bathurst, R. J. (2007). "Development of K-stiffness method for geosynthetic reinforced soil walls constructed with c-ϕ soils." *Can. Geotech. J.*, 44(12), 1391–1416.

Mualem, Y. (1976). "A new model for predicting hydraulic conductivity of unsaturated porous media." *Water Resour. Res.*, 12(3), 513–522.

NCMA (National Concrete Masonry Association). (2009). *Design manual for segmental retaining walls*, 3rd Ed., Herndon VA.

NOAA (National Oceanic and Atmospheric Administration). (2013). "Regional climate trends and scenarios for the U.S. national climate assessment." *NOAA Technical Rep. NESDIS 142*, U.S. Dept. of Commerce, National Oceanic and Atmospheric Administration, National Environmental Satellite, Data, and Information Service, Washington, DC.

NRC. (2008). *Potential impacts of climate change on U.S. transportation*, Committee on Climate Change and U.S. Transportation, Transportation Research Board, Division on Earth and Life Studies, Washington, DC, 296.

NRC. (2013). *Abrupt impacts of climate change: Anticipating surprises*, Committee on Understanding and Monitoring Abrupt Climate Change and Its Impacts, Board on Atmospheric Sciences and Climate, Division on Earth and Life Studies, Washington, DC, 250.

PLAXIS version 2016.01 [Computer software]. Plaxis bv, Delft, Netherlands.

Portelinha, F. H. M., Bueno, B. S., and Zornberg, J. G. (2013). "Performance of nonwoven geotextile-reinforced walls under wetting conditions: Laboratory and field investigations." *Geosynth. Int.*, 20(2), 90–104.

Riccio, M., Ehrlich, M., and Dias, D. (2014). "Field monitoring and analyses of the response of a block-faced geogrid wall using fine-grained tropical soils." *Geotext. Geomembr.*, 42(2), 127–138.

Richards, L. A. (1931). "Capillary conduction of liquids through porous mediums." *J. Appl. Phys.*, 1(5), 318–333.

Robinson, J. D., and Vahedifard, F. (2016). "Weakening mechanisms imposed on California's levees under multiyear extreme drought." *Clim. Change*, 137(1), 1–14.

Robinson, J. D., Vahedifard, F., and AghaKouchak, A. (2017). "Rainfall-triggered slope instabilities under a changing climate: Comparative study using historical and projected precipitation extremes." *Can. Geotech. J.*, 54(1), 117–127.

Simonovic, S. P., and Peck, A. (2009). *Updated rainfall intensity duration frequency curves for the City of London under the changing climate*, Dept. of Civil and Environmental Engineering, Univ. of Western Ontario, London.

Sugahara, S., Da Rocha, R. P., and Silveira, R. (2009). "Non-stationary frequency analysis of extreme daily rainfall in Sao Paulo, Brazil." *Int. J. Climatol.*, 29(9), 1339–1349.

Taylor, K. E., Stouffer, R. J., and Meehl, G. A. (2012). "An overview of CMIP5 and the experiment design." *Bull. Am. Meteorol. Soc.*, 93(4), 485–498.

Taylor, R. G., et al. (2013). "Ground water and climate change." *Nat. Clim. Change*, 3(4), 322–329.

Thuo, J. N., Yang, K. H., and Huang, C. C. (2015). "Infiltration into unsaturated reinforced slopes with nonwoven geotextile drains sandwiched in sand layers." *Geosynthetics Int.*, 22(6), 457–474.

Trenberth, K. E. (2011). "Changes in precipitation with climate change." *Clim. Res.*, 47(1), 123–138.

USGCRP (U.S. Global Change Research Program). (2009). *Global climate change impacts in the United States*, Cambridge University Press, Washington, DC.

Vahedifard, F., AghaKouchak, A., and Jafari, N. H. (2016a). "Compound hazards yield Louisiana flood." *Science*, 353(6306), 1374.

Vahedifard, F., AghaKouchak, A., and Robinson, J. D. (2015a). "Drought threatens California's levees." *Science*, 349(6250), 799.

Vahedifard, F., Leshchinsky, B., Mortezaei, K., and Lu, N. (2015b). "Active earth pressures for unsaturated retaining structures." *J. Geotech. Geoenviron. Eng.*, 10.1061/(ASCE)GT.1943-5606.0001356, 04015048.

Vahedifard, F., Leshchinsky, B. A., Sehat, S., and Leshchinsky, D. (2014). "Impact of cohesion on seismic design of geosynthetic-reinforced earth structures." *J. Geotech. Geoenviron. Eng.*, 10.1061/(ASCE)GT.1943-5606.0001099, 04014016.

Vahedifard, F., Leshchinsky, D., Mortezaei, K., and Lu, N. (2016c). "Effective stress-based limit equilibrium analysis for homogeneous unsaturated slopes." *Int. J. Geomech.*, 10.1061/(ASCE)GM.1943-5622.0000554, D4016003.

Vahedifard, F., Mortezaei, K., Leshchinsky, B. A., Leshchinsky, D., and Lu, N. (2016b). "Role of suction stress on service state behavior of geosynthetic-reinforced soil structures." *Transp. Geotech.*, 8, 45–56.

Vahedifard, F., and Robinson, J. D. (2016). "A unified method for estimating the ultimate bearing capacity of shallow foundations in variably saturated soils under steady flow." *J. Geotech. Geoenviron. Eng.*, 10.1061/(ASCE)GT.1943-5606.0001445, 04015095.

Vahedifard, F., Robinson, J. D., and AghaKouchak, A. (2016d). "Can protracted drought undermine the structural integrity of California's earthen levees?" *J. Geotech. Geoenviron. Eng.*, 10.1061/(ASCE)GT.1943-5606.0001465, 02516001.

Valentine, R. J. (2013). "An assessment of the factors that contribute to the poor performance of geosynthetic-reinforced earth retaining walls." *Proc., Int. Symp. on Design and Practice of Geosynthetic-Reinforced Soil Structures*, H. I. Ling, et al. eds., DEStech Publication, Inc., Lancaster, PA, 318–327.

van Genuchten, M. T. (1980). "A closed-form equation for predicting the hydraulic conductivity of unsaturated soils." *J. Soil Sci.*, 44(5), 892–898.

Vardon, P. J. (2015). "Climatic influence on geotechnical infrastructure: A review." *Environ. Geotech.*, 2(3), 166–174.

Wahl, T., Jain, S., Bender, J., Meyers, S. D., and Luther, M. E. (2015). "Increasing risk of compound flooding from storm surge and rainfall for major US cities." *Nat. Clim. Change*, 5(12), 1093–1097.

Yoo, C. (2013). "Effect of rainfall on performance of geosynthetic reinforced soil wall using stress-pore pressure coupled analysis." *Proc., 2013 Geo-Congress: Stability and Performance of Slopes and Embankments III*, ASCE, Reston, VA, 566–573.

Yoo, C., and Jung, H. (2006). "Case history of geosynthetic reinforced segmental retaining wall failure." *J. Geotech. Geoenviron. Eng.*, 10.1061/(ASCE)1090-0241(2006)132:12(1538), 1538–1548.